Direct Measurement of Nonequilibrium Electron-Energy Distributions in Subpicosecond Laser-Heated Gold Films

W. S. Fann,[1] R. Storz,[1] H. W. K. Tom,[1] and J. Bokor[2]
[1]*AT&T Bell Laboratories, Holmdel, New Jersey 07733*
[2]*AT&T Bell Laboratories, Murray Hill, New Jersey 07974*

(Received 6 September 1991)

The electron-energy distribution in a gold film was measured with ~700 fs time-resolved photoemission spectroscopy following laser heating by a 400 fs visible laser pulse. The measured distribution can be fitted by the Fermi-Dirac function at an elevated temperature except within 800 fs of the heating pulse (time-resolution limited), when a reproducible departure is observed. As a result, the relaxation of nonequilibrium electrons was found to be inadequately described by the standard electron-phonon coupling model.

PACS numbers: 78.47.+p

The fact that the electronic heat capacity of metals is 1 to 2 orders of magnitude smaller than the lattice heat capacity has led to many investigations of nonequilibrium phenomena in metals with subpicosecond lasers. Model calculations suggest that it should be possible to heat the electron gas to a temperature T_e of up to several thousand K for a few ps while keeping the lattice temperature T_l relatively cold [1,2]. Observing the subsequent equilibration of the electronic system with the lattice allows one to directly study electron-phonon coupling under various and unusual conditions [3]. Detailed understanding of the electron-electron (*e-e*) and electron-phonon relaxation mechanisms should also provide greater insight into chemical reactions [4] and phase transitions [5] induced by ultrashort laser pulses. Several groups have undertaken such investigations by relating dynamic changes in the optical constants (reflectivity, transmissivity) to relative changes in electronic temperature [6-10]. However, no *direct* measurement of electron temperature has been reported so far. More importantly, the fact that T_e is a valid concept only if the electron gas is fully thermalized has often been ignored. Direct measurement of the dynamics of the electron distribution by photoemission spectroscopy provides a much more complete picture of the mechanisms of relaxation of such highly nonequilibrium systems. Not only are difficulties of relating the dynamic changes of the optical constants to the electron temperature removed but the direct measurement of the energy distribution allows for the experimental investigation of the usual implicit assumption that the hot electron gas is immediately and fully thermalized.

In this Letter we report the direct measurement of the electron-energy-distribution dynamics in gold films using subpicosecond laser photoemission spectroscopy. A 674-nm-wavelength (1.84 eV photon energy) pump pulse of 400-fs duration was used to excite a 300-Å-thick polycrystalline gold film. The heating pulse fluence varied from 0.4 to 1.6 mJ/cm^2 and 15% of the light was absorbed. The laser system consists of a dual-jet synchronously pumped dye laser amplified to 200 μJ/pulse by a 100-Hz excimer-laser-pumped dye amplifier system. The 225-nm probe pulse (5.52 eV photon energy) was produced by first frequency doubling the 674-nm amplified dye laser output in a potassium-dihydrogen-phosphate (KDP) crystal and subsequently frequency mixing the 674-nm radiation with the 337-nm second-harmonic radiation in a beta-barium-borate (BBO) crystal. The probe pulse duration was measured to be 700 fs by cross correlation with the visible 674-nm pulse. The photoemission spectrum produced by the probe pulse was measured by the time-of-flight technique. Only electrons emitted in a ±4° cone angle from the sample surface normal were detected. We used a relatively large probe beam spot size, ~1 mm^2, to eliminate space-charge broadening of the spectrum while maintaining an adequate photoelectron count rate. Since the work function of gold is 5.1 eV, the 5.52-eV probe photons produce photoelectrons by single-photon photoemission.

We chose gold because it has a small electronic heat capacity so the electronic temperature rise for a given laser intensity is relatively large. Secondly, the electronic structure of gold is relatively simple [11]. Since the *d* bands lie 2 eV below the Fermi energy E_F, gold may be considered as a free-electron metal for energies $E_F \pm 1$ eV, the regime probed in this experiment. The use of thin films eliminates the effect of electronic heat diffusion, simplifying the data analysis.

In Fig. 1 we show spectra for several pump-probe time delays. The Fermi "smearing" effect is clearly observed. To directly compare the data with the Fermi-Dirac (FD) function, the spectrum plotted is the electron counts per unit energy, $dN(E)/dE$, divided by the normalized joint density of states (JDOS) shown in the inset. The JDOS takes into account the energy-dependent differences in initial and final density of states and in oscillator strengths. It also accounts for any energy dependence in the transmission function of the time-of-flight electron spectrometer. To derive the JDOS, the electron gas was excited above 1000 K by a strong pump pulse and the resulting spectra were fitted by the FD function. The JDOS was taken as the ratio between the measured spectrum and the best-fit FD function at the shortest time delay such that all subsequent spectra could be fitted by the same JDOS times a FD function. In the region of interest, the relative variation of the JDOS is < 20%.

Figure 1 also shows the best fit of the FD function to

© 1992 The American Physical Society

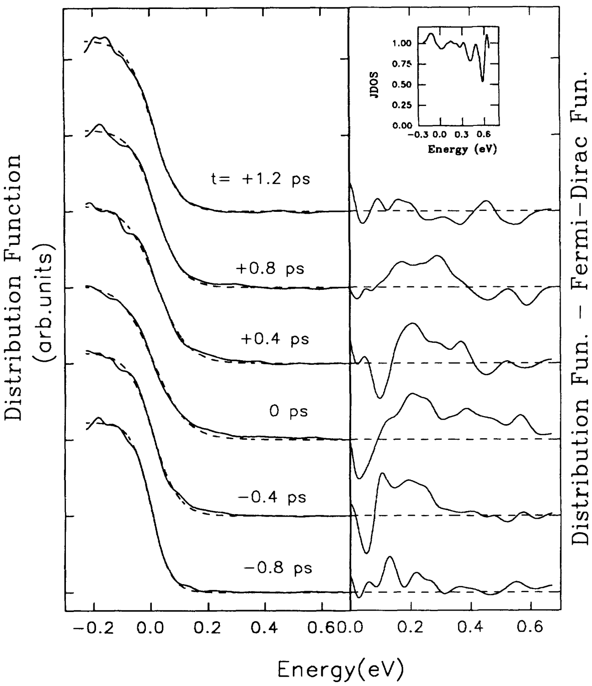

FIG. 1. Photoelectron spectra (solid line) and least-squares best fits by the Fermi-Dirac function (dashed line) for several different time delays. Inset: The spectra normalized to the joint density of states. The difference between the normalized spectra and the Fermi-Dirac function is shown 10× in the right-hand panel. The fits correspond to electron temperatures of 380, 483, 625, 582, 508, and 490 K for $t=-0.8$, -0.4, 0.0, +0.4, +0.8, and +1.2 ps, respectively.

the normalized data. We used a nonlinear least-squares fitting routine in which the chemical potential μ, electron temperature T_e, and an overall vertical scale factor are used as fitting parameters. The random variation of the best-fit value of μ for spectra taken at different intensities and time delays is around 10 meV. The fitted temperature for the $t=-0.8$ ps spectrum is 360 K, which is higher than the actual substrate temperature, 300 K. This is due to ∼30 meV energy resolution of the time-of-flight electron spectrometer which sets an instrumental limit on the lowest temperature which can be measured [12]. Because of the typical signal-to-noise ratio and the details of the data analysis procedures, the temperature accuracy for all fits was determined to be ±30 K. The best-fit temperatures are indicated in the caption to Fig. 1. The quality of the fits is quite good for the $t=-0.8$ and +1.2 ps spectra. In fact, for all time delays > 0.8 ps, the spectra are well fitted by the FD function.

On the other hand, there is a reproducible and systematic deviation from a simple FD distribution for the $t=0$ and ±0.4 ps spectra. For example, the best-fit temperature at $t=0$ ps is 625 K, but there is a large discrepancy from the FD function in the range from 0 to +0.5 eV. The deviation is explicitly shown on the right-hand side of Fig. 1. We believe this deviation arises due to the finite time required for the "nascent" electrons to equilibrate to a FD distribution and shall refer to it as a "hot tail." A similar deviation below E_F due to "hot holes" is expected as well; however, we were unable to investigate these due to a low-energy cutoff in our spectra. By nascent, we mean the electron-energy distribution as created by the direct absorption of the photons prior to any scattering, which, in principle, extends from E_F to $E_F+1.8$ eV.

By explicitly extracting the JDOS and normalizing it out of the data, we eliminated the possibility that the hot tail could be due to a density-of-states effect. We also considered the possibility that the hot tail arises from the laser pulse-to-pulse energy fluctuation. By calculating a sum of FD functions at different temperatures, weighted by the measured laser pulse-energy distribution, we found that the spectrum is well described by a single FD function with the mean temperature. No hot tail could be produced in this way. We ruled out the possibility that the hot tail is related to inhomogeneities in the laser beam profile by carefully producing a nearly flattopped beam profile on target. We may also rule out the possibility that the hot tail is due to coherent two-photon photoemission from the pump and probe because such processes would produce an electron distribution anomaly that reflected the nascent distribution and should therefore be essentially *flat* from E_F to $E_F+1.8$ eV. The data clearly show no deviation. We therefore conclude that the hot tail is genuinely a signature of nonthermalized electrons.

We now examine the relaxation dynamics of the electron temperature and how well it can be described by the usual electron-phonon coupling model [1,2]. In this model one describes the metal as two coupled subsystems, one for electrons and one for phonons. Each subsystem is in local equilibrium so the electrons are characterized by a FD distribution at temperature T_e and the phonon distribution is characterized by a Bose-Einstein distribution at the lattice temperature T_l. The coupling between the two systems occurs via the electron-phonon interaction, characterized by an exchange of energy at a rate proportional to T_e-T_l. The time evolution of the energies in the two subsystems is given by the coupled differential equations

$$C_e(T_e)\frac{\partial T_e}{\partial t}=\nabla_x(\kappa\nabla_x T_e)-G(T_e-T_l)+P(x,t)\,, \qquad (1a)$$

$$C_l\frac{\partial T_l}{\partial t}=G(T_e-T_l)\,. \qquad (1b)$$

In Eqs. (1a) and (1b), T_e and T_l are the electron and lattice temperatures, $C_e(T_e)$ is the temperature-dependent electronic heat capacity, C_l is the lattice heat capacity, κ is the thermal conductivity, G is the electron-phonon coupling constant, and $P(x,t)$ is the energy density per unit time absorbed from the incident laser beam.

In Fig. 2 we show the electron temperature (obtained

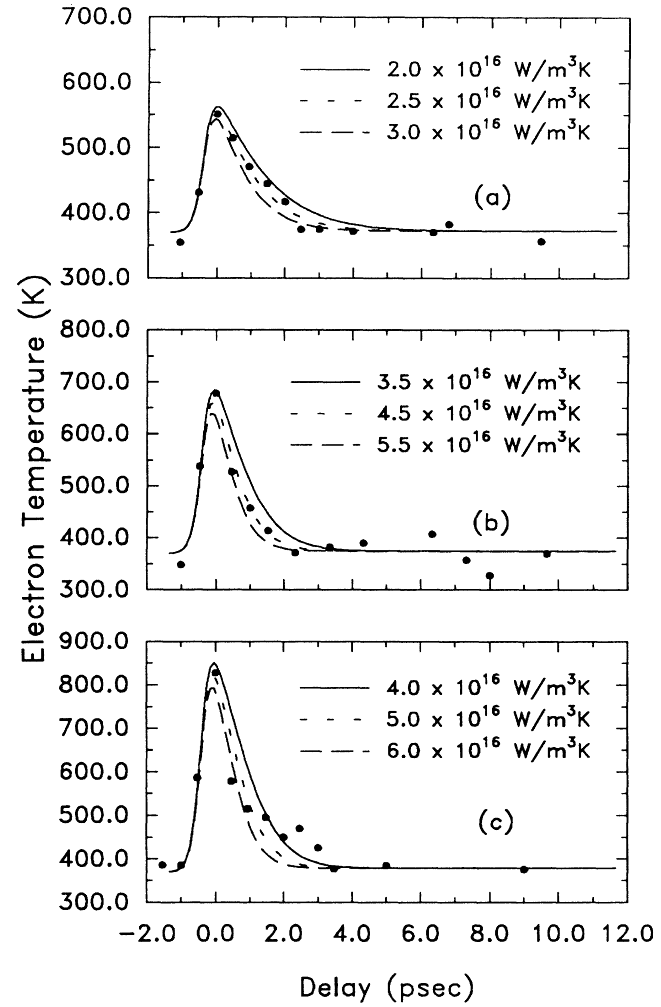

FIG. 2. Time dependence of best-fit electron temperature for three heating laser pulse fluences. Fits used the values of G shown and heating laser fluences of (a) measured 0.09 ± 0.03 and fitted 0.10 mJ/cm^2, (b) measured 0.16 ± 0.03 and fitted 0.21 mJ/cm^2, and (c) measured 0.2 ± 0.06 and fitted 0.37 mJ/cm^2.

by the best fit with the photoemission spectra) versus time delay for measured absorbed laser fluences of 0.09 ± 0.03, 0.16 ± 0.03, and 0.2 ± 0.06 mJ/cm^2. In addition, we show the calculated electron temperatures obtained by numerically solving Eqs. (1). For gold $C_e = \gamma T_e$ with $\gamma = 71.5$ J m^{-3}K^{-2}, $C_l = 3.5 \times 10^6$ J m^{-3}K^{-1}, and $\kappa = 310$ W m^{-1}K^{-1}. $P(x,t)$ was proportional to the laser intensity pulse shape and to the exponential depth dependence of the optical absorption. The equations were solved in one dimension and with the boundary conditions appropriate for the thin film. Because of difficulties in experimentally determining the precise location of $t = 0$ ps (perfect overlap of the pump and probe pulses), we chose the $t = 0$ ps delay point to correspond to the time with maximum electron temperature for both the data and calculation. The values of the absorbed fluence used in the calculation in Figs. 2(b) and 2(c) are somewhat higher than the measured fluence. However, we note that the choice of the absorbed fluence used in the fit mainly affects the peak temperature and the overall decay time of the electron temperature slightly, but does not change the form of the decay curve.

As one sees immediately, there is no single value of G that fits all three sets of data. Best fits are obtained for values in the range $(2.5\text{–}6) \times 10^{16}$ W m^{-3}K^{-1}. In particular, for the highest fluence [Fig. 2(c)], the decay is almost biexponential. The early part of the curve requires $G \approx 6 \times 10^{16}$ W m^{-3}K^{-1} and a much lower value for the later part of the curve. However, once the FD distribution is obtained (in these experiments $t > 800$ fs), a single value of $G = (3.0 \pm 0.5) \times 10^{16}$ W m^{-3}K^{-1} can be used to fit all of the data.

This is not a completely surprising result since Eq. (1a) does not properly take into account (1) the finite time for the nascent electrons to relax to the FD distribution, and (2) the possibility of an increased rate of energy transfer to the lattice when the electron-energy distribution is non-FD type. In order for Eqs. (1) to be valid, the time required to relax to the FD distribution must be much faster than the time required for electron-phonon scattering so no energy is transferred to the lattice. This assumption is clearly not valid for our experimental conditions. The rapid drop of the "best-fit" FD temperature from 830 to 580 K within 500 fs in Fig. 2(c) directly shows that a substantial amount of energy is transferred from the electron subsystem to the lattice subsystem during the transition from the nascent to the FD distribution. On the other hand, once the system is thermalized, the relaxation dynamics is well described by the coupling model with a single value of G.

The relaxation of nonthermalized electrons to a thermal FD distribution is a complicated many-body problem. Landau's Fermi-liquid theory [13] provides a starting point to analyze the problem. According to Fermi-liquid theory, the single-particle lifetime above the Fermi level scales as $(E - E_F)^{-2}$. The higher the energy, the faster the relaxation time, and a particle just at the Fermi level should have an infinite lifetime. Sze, Moll, and Sugano [14] have used internal photoemission to measure the mean free path of electrons 1 eV above E_F in gold. These authors conclude that the e-e scattering mean free path is around 1000 Å at this energy. For an electron energy 0.4 eV above the Fermi energy, the scattering length should be around 0.6 μm according to the simple scaling law. Since the Fermi velocity is about 10^8 cm/s, the e-e scattering time for 0.4-eV electrons is about 0.6 ps. This result is consistent with the present measurements. Based on the data in Fig. 1, we estimate that population in the hot tail in the neighborhood of +0.4 eV represents of the order of 2% of the available density of states. Based on the absorbed fluence, the number of electrons that are initially excited by a photon is approximately 3×10^{20} cm^{-3} which would fill 1% of the DOS between E_F and $E_F + 1.8$ eV, in the absence of relaxation. The fact that these numbers are comparable implies that the lifetime of the 0.4-eV electrons is comparable to the UV pulse width, e.g., ~700 fs. If the lifetime of the electrons were much shorter, say, 70 fs, then we would expect to see $\frac{1}{10}$th the signal. This is probably why we do not observe the hot tail much beyond ~0.4 eV: Electrons at those energies relax faster than we can observe with our time resolution.

These results also help to clarify a previous experiment on femtosecond electronic heat transport dynamics in thin gold films [8]. In that experiment, electronic "heat" was found to flow from the front to back of a thin gold film in a time which scaled linearly with film thickness, indicating nondiffusive, ballistic transport. This suggested that there was a component of nonthermalized electrons which live long enough to cross a 1000–2000-Å-thick film. We can now understand that these are the electrons comprising the hot tail which we observe in the present experiment.

A great deal of information about the electron thermalization process in semiconductors, especially GaAs, has been obtained in the last decade. For example, the carrier-carrier thermalization time in bulk GaAs was found to be [15] ~300 fs for an electron density of 3×10^{17} cm^{-3} and ~100 fs for quantum wells [16]. Naively, one might expect the scattering time to be dramatically shorter at the electron densities characteristic of metals. However, degeneracy has a profound effect on *e-e* scattering. Because of the combination of screening and degeneracy, the *e-e* scattering rate indeed increases with density for low densities, but peaks and actually decreases again for high densities as degeneracy is reached [17].

In summary, we have demonstrated that photoemission spectroscopy could be used to measure the electron-energy distribution in laser-heated metals on a subpicosecond time scale. It was confirmed that the coupling between the electrons and lattice is weak on this time scale, hence it is possible to highly excite the electron gas while keeping the lattice relatively cold. However, the hot electron spectra could not be fitted by a FD distribution at the earliest times indicating a finite relaxation time for the electrons from their nascent to FD distribution. As a result, an electron temperature cannot be defined in this phase of the process and hence the electron-phonon coupling model of Anisimov, Kapeliovich, and Perelman [2], commonly used to analyze laser-heating experiments, fails on the subpicosecond time scale. Experiments which relate transient optical reflectivity changes to electron temperature may also need to be reexamined in light of our results. The detailed dynamics of the relaxation of the nascent distribution to Fermi-Dirac were not resolved and improved time resolution will be required in order to do so. Such studies are currently in progress.

We are pleased to acknowledge fruitful discussions with H. Roskos, A. Chang, W. Knox, S. Schmitt-Rink, J. Prybyla, S. Ullah, and A. F. J. Levi.

[1] M. I. Kaganov, I. M. Lifshitz, and L. V. Tanatarov, Zh. Eksp. Teor. Fiz. **31**, 2232 (1956) [Sov. Phys. JETP **4**, 173 (1957)].

[2] S. I. Anisimov, B. L. Kapeliovich, and T. L. Perelman, Zh. Eksp. Teor. Fiz. **66**, 776 (1974) [Sov. Phys. JETP **39**, 375 (1975)].

[3] P. B. Allen, Phys. Rev. Lett. **59**, 1460 (1987).

[4] J. A. Prybyla, T. F. Heinz, J. A. Misewich, M. M. T. Loy, and J. H. Glownia, Phys. Rev. Lett. **64**, 1537 (1990); F. Budde, T. F. Heinz, M. M. T. Loy, J. A. Misewich, F. de Rougemont, and H. Zacharias, Phys. Rev. Lett. **66**, 3024 (1991).

[5] C. V. Shank, R. Yen, and C. Hirlimann, Phys. Rev. Lett. **50**, 454 (1983); **51**, 900 (1983); H. W. K. Tom, G. D. Aumiller, and C. H. Brito-Cruz, Phys. Rev. Lett. **60**, 1438 (1988).

[6] H. E. Elsayed-Ali, T. B. Norris, M. A. Pessot, and G. A. Mourou, Phys. Rev. Lett. **58**, 1212 (1987).

[7] R. W. Schoenlien, W. Z. Lin, J. G. Fujimoto, and G. L. Eesley, Phys. Rev. Lett. **58**, 1680 (1987).

[8] S. D. Brorson, J. G. Fujimoto, and E. P. Ippen, Phys. Rev. Lett. **59**, 1962 (1987).

[9] H. E. Elsayed-Ali, J. Juhasz, G. O. Smith, and W. E. Bron, in *Ultrafast Phenomena VII*, edited by C. B. Harris, E. P. Ippen, G. A. Mourou, and A. H. Zewail (Springer-Verlag, Berlin, 1990).

[10] S. D. Brorson, A. Kazeroonian, J. S. Moodera, D. W. Face, T. K. Cheng, E. P. Ippen, M. S. Dresselhaus, and G. Dresselhaus, Phys. Rev. Lett. **64**, 2172 (1990).

[11] N. E. Christensen, and B. O. Seraphin, Phys. Rev. B **4**, 3321 (1971); W. F. Krolikowski and W. E. Spicer, Phys. Rev. B **1**, 478 (1970).

[12] The lowest fitted temperatures for unheated samples were consistently in the 330–380-K range.

[13] D. Pine and P. Nozieres, *The Theory of Quantum Liquids* (Benjamin, New York, 1966).

[14] S. M. Sze, J. L. Moll, and T. Sugano, Solid State Electron. **7**, 509 (1964); S. M. Sze, C. R. Crowell, G. P. Carey, and E. E. Labate, J. Appl. Phys. **37**, 2690 (1966).

[15] J. L. Oudar, D. Hulin, A. Migus, A. Antonetti, and F. Alexandre, Phys. Rev. Lett. **55**, 2074 (1985).

[16] W. H. Knox, C. Hirliman, D. A. B. Miller, J. Shah, D. S. Chemla, and C. V. Shank, Phys. Rev. Lett. **56**, 1191 (1986).

[17] A. F. J. Levi, Electronic Lett. **124**, 1273 (1988).